Paleomagnetism and magnetic fabrics of Mio-Pliocene hypabyssal rocks of the Combia event, Colombia: tectonic implications

VICTOR A. PIEDRAHITA[1], ROBERTO S. MOLINA-GARZA[2], GLORIA M. SIERRA[1] AND JOSÉ F. DUQUE-TRUJILLO[1]

1 Departamento de Ciencias de la Tierra, Universidad EAFIT, Medellín, Colombia (vpiedra2@eafit.edu.co)

2 Centro de Geociencias, Universidad Nacional Autónoma de México, Blvd. Juriquilla 3001, Querétaro, Mexico

Received: June 21, 2016; Revised: January 10, 2017; Accepted: March 15, 2017

ABSTRACT

Mio-Pliocene hypabyssal rocks of the Combia event in the Amagá basin (NW Andes-Colombia), contain a deformational record of the activity of the Cauca-Romeral fault system, and the interaction of terranes within the Choco and northern Andean blocks. Previous paleomagnetic studies interpreted coherent counterclockwise rotations and non-coherent modes of rotation about horizontal axes for the Combia intrusives. However, rotations were determined from in-situ paleomagnetic directions and the existing data set is small. In order to better understand the deformational features of these rocks, we collected new paleomagnetic, structural, petrographic and magnetic fabric data from well exposed hypabyssal rocks of the Combia event. The magnetizations of these rocks are controlled by a low-coercivity ferromagnetic phase. Samples respond well to alternating-field demagnetization isolating a magnetization component of moderate coercivity. These rocks do not have ductile deformation features. Anisotropy of magnetic susceptibility and morphotectonic analysis indicate that rotation about horizontal axes is consistently to the south-east, suggesting the need to apply a structural correction to the paleomagnetic data. The relationships between magnetic foliations and host-rock bedding planes indicate tectonic activity initiated before ~10 Ma. We present a mean paleomagnetic direction (declination $D = 342.8°$, inclination $I = 12.1°$, 95% confidence interval $\alpha_{95} = 12.5°$, precision parameter $k = 8.6$, number of specimens $n = 18$) that incorporates structural corrections. The dispersion $S = 27°$ of site means cannot be explained by secular variation alone, but it indicates a counterclockwise rotation of $14.8° \pm 12.7°$ relative to stable South America. Paleomagnetic data within a block bounded by the Sabanalarga and Cascajosa faults forms a more coherent data set ($D = 336.5°$, $I = 17.4°$, $\alpha_{95} = 11.7°$, $k = 12.5$, $n = 14$), which differs from sites west of the Sabanalarga fault and shows a rotation about a vertical axis of $20.2° \pm 10.7°$. Deformation in the Amagá basin may be tentatively explained by the obduction of the Cañas Gordas terrane over the northwestern margin of the northern Andean block. However, it can also be related to the local effects of the Cauca-Romeral fault system.

Stud. Geophys. Geod., 61 (2017), 772–800, DOI: 10.1007/s11200-016-0372-0

K e y w o r d s: Combia event, Andean tectonics, Cañas Gordas terrane, Cauca-Romeral fault system

1. INTRODUCTION

The inter-Andean valley between the Western and Central Cordilleras of Colombia is characterized by strike-slip tectonics due to the activity along the Cauca-Romeral fault system, that affects an older assemblage of tectonostratigraphic terranes. The region is also occupied by a series of sedimentary basins, which include the Amagá and Cauca-Patía basins. These basins are extensional in nature (*Acosta, 1978*; *McCourt, 1984*; *Alfonso et al., 1994*; *Sierra and Marín-Cerón, 2011*) and within them, changes in sedimentation and structural regime may contain a record of activity along the Cauca-Romeral fault system (*Sierra, 1994*; *Sierra and Marín-Cerón, 2011*; *Sierra et al., 2012*).

The Amagá basin is located in the northern region of the inter-Andean valley, and is filled by Cenozoic sedimentary and volcano-sedimentary rocks. The sedimentary infill of the Amagá basin is intruded by hypabyssal rocks in the central and southern parts of the basin (Fig. 1) (*Calle and González, 1980*; *Sierra and Marín-Cerón, 2011*). These hypabyssal rocks were originated by a Mio-Pliocene magmatic event that has been genetically linked to the Cauca-Romeral fault system (*Marriner and Millward, 1984*; *López et al., 2006*). This event is called the Combia event and it produced a succession of volcanic and hypabyssal intrusive rocks. Paleomagnetic studies in the hypabyssal

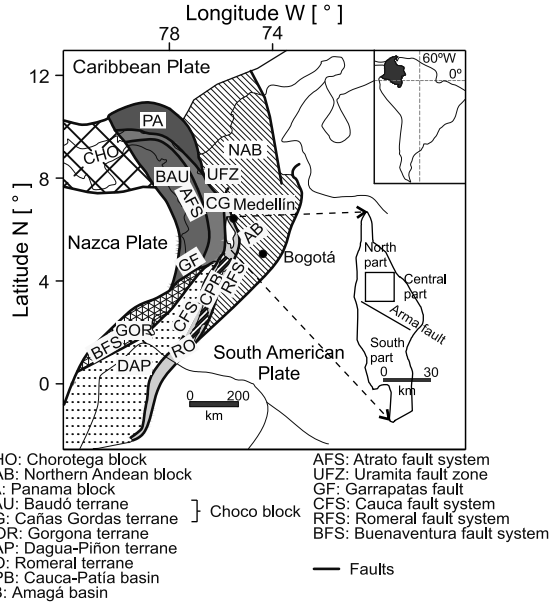

Fig. 1. Tectonic framework and geological map of the northwestern Andes, including terranes, principal faults, and inter-Andean basins (*Cediel et al., 2003*; *Sierra and Marín-Cerón, 2011*). Additionally, the study area is shown in the central part of the Amagá basin.

intrusive rocks of the Combia event were conducted with the objective of identifying the effects of the Cauca-Romeral fault system within the Amagá basin (e.g., *MacDonald, 1980*; *MacDonald et al., 1996*).

MacDonald (1980) presented paleomagnetic data for four intrusive bodies of the Combia event located in the central part of the Amagá basin (Fig. 2). The paleomagnetic directions reported are characterized by in-situ magnetic declinations towards the NW (304° to 336°) and magnetic inclinations with values between −14.9° and 60°. According to *MacDonald (1980)* and *MacDonald et al. (1996)*, the paleomagnetic directions in the

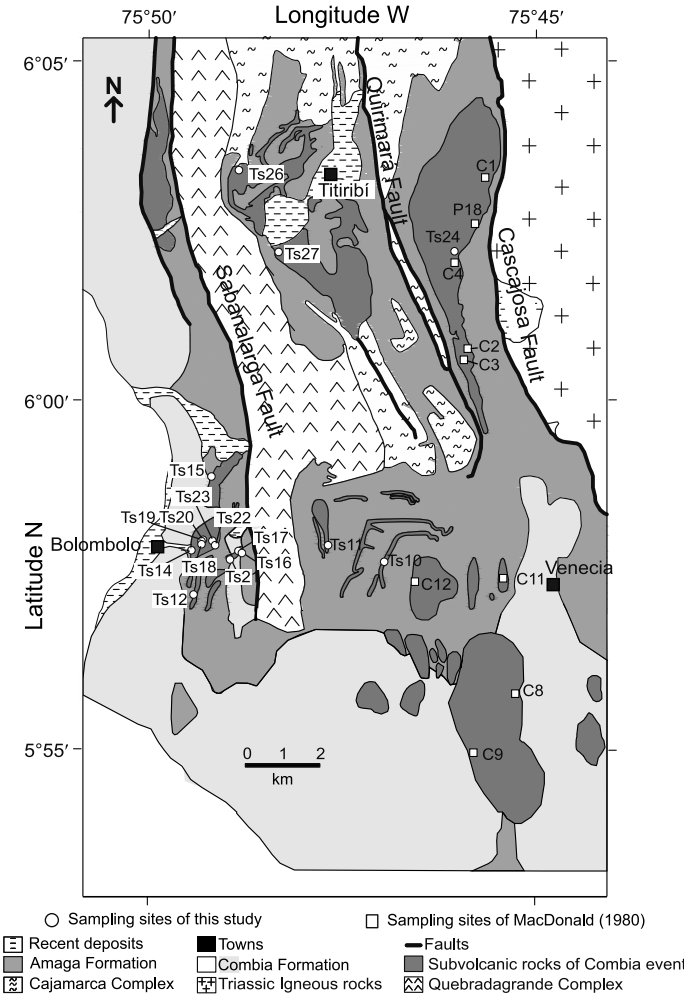

Fig. 2. Geological map of the study area (*Grosse, 1926*; *Calle et al., 1980*) including sampling sites used in this study and sampling sites used by *MacDonald (1980)*.

hypabyssal rocks in the central part of the Amagá basin can be explained by two modes of rotation: a coherent mode of rotation about a vertical axis, and a non-coherent mode of rotation about horizontal axes. These authors also obtained paleomagnetic data in seven hypabyssal bodies belonging to the Combia event in the southern part of the Amagá basin; but in this case, the paleomagnetic directions do no show systematic deviations from the expected direction. *MacDonald (1980)* and *MacDonald et al. (1996)* suggested that post Mio-Pliocene activity of the Romeral system and associated faults in the central part of the Amagá basin is related to a coherent rotation behavior, with counterclockwise rotations of approximately 35° about a vertical axis and local tilting. On the other hand, the shift in the paleomagnetic directions found in the southern part of the Amagá basin was linked to a major change in the trend of the Romeral fault (*MacDonald et al., 1996*).

The rotations of hypabyssal intrusive rocks of the Combia event have been attributed to the obduction of the Cañas Gordas terrane over the northwestern terranes of the north Andean block (*Cediel et al., 2003*). However, the conclusions of *MacDonald (1980)* and *MacDonald et al. (1996)* are based on the interpretation of in-situ directions, and implicitly reflect the assumption that secular variation is sufficiently well averaged. In order to provide a more thorough evaluation of these assumptions, our study presents new paleomagnetic data for hypabyssal rocks in the central part of the Amagá basin revisiting one of the localities studied by *MacDonald (1980)*. Additionally, we show new field relationships and morphotectonic analyses, petrographic, rock magnetic, and magnetic fabric data with the goal of a better characterization of the deformation imprinted by the Cauca-Romeral fault system on the hypabyssal intrusives of the Combia event, and its relationship with the interaction between different tectonic blocks and terranes in the northwestern Andes.

2. REGIONAL GEOLOGY

The geology of northern South America is the result of interactions between three major plates: Caribbean, Nazca and South America. Different tectonic blocks are located within the region where these plates interact. This is the case of the Chorotega, Panama, and Choco blocks (Fig. 1) (*Molnar and Sykes, 1969*). The Choco block was accreted onto northwestern South America, and is bounded to the east by the Uramita fault zone and to the south by the Garrapatas fault (?) (*Duque-Caro, 1990*; *Mann and Corrigan, 1990*; *Mann and Kolarsky, 1995*; *Cediel et al., 2003*; *Vargas-Jiménez and Durán-Tovar, 2005*). The Choco block is represented by the Baudó and Cañas Gordas terranes, which are oceanic terranes that were accreted onto the western margin of the northern Andean block during the Miocene (*Duque-Caro, 1990*; *Cediel et al., 2003*; *Montes et al., 2012, 2015*). The northern Andean block is a tectonic block geologically distinct from the rest of the Andes Cordillera (*Gansser, 1973*; *Shagam, 1975*; *Cediel et al., 2003*). It is characterized by N-S-trending faults that separate oceanic terranes such as the Romeral, Dagüa-Piñon, and Gorgona terranes (Fig. 1) (*Cediel et al., 2003*).

The Romeral terrane is bounded to the east by the Romeral fault, which is an ancient suture that extends from Ecuador to central Colombia; it separates oceanic crust to the west from continental crust on the eastern margin of South America (*Case et al., 1971*). This suture has been interpreted as a rheologically weak zone that underwent dextral

displacement during the Paleocene and the Miocene (*Hutchings et al., 1981*; *Ego and Sébrier, 1995*; *Chicangana, 2005*). The Romeral fault was originated by the oblique collision and dextral displacement of the Caribbean plate to the northeast in the Early Cretaceous (*Pindell and Kennan, 2009*). The Dagüa-Piñon terrane is located to the west of the Romeral terrane. These terranes are bounded by the Cauca fault, which is also a suture characterized by dextral displacements and has its behavior linked to the Romeral fault (*Kammer, 1993*; *Ego and Sébrier, 1995*). The Dagüa-Piñon terrane is bounded on the west by the Buenaventura fault system, which is characterized by its dextral offset. This fault system forms the eastern boundary of the Gorgona terrane, yet another oceanic terrane located on the western margin of the northern Andean block (Fig. 1) (*Cediel et al., 2003*).

The Mio-Pliocene interaction between tectonic blocks, and the subsequent reactivation of faults, have significantly modified the geology of northern South America (*Duque-Caro, 1990*; *Mann and Corrigan, 1990*; *Van der Hilst and Mann, 1994*; *Taboada et al., 2000*; *Trenkamp et al., 2002*; *Cediel et al., 2003*; *Montes et al., 2012, 2015*). Some of these changes are recorded in the volcanic activity and deformation within the Amagá basin (*Duque-Caro, 1990*; *Cediel et al., 2003*; *Sierra and Marín-Cerón, 2011*). This Cenozoic sedimentary basin is located in the Romeral terrane, and is bounded on the east by the Romeral fault and on the west by the Cauca fault (*Barrero et al., 2007*; *Sierra and Marín-Cerón, 2011*). The Cauca and Romeral faults integrate the Cauca-Romeral fault system (*Kammer, 1993*), which controls the deformation of the rocks located within the Amagá basin, and has an associate Miocene magmatism recorded in this basin.

Miocene magmatism in the Central and Western Cordilleras of Colombia is characterized by subduction-related products (*Marriner and Millward, 1984*; *Leal-Mejía, 2011*). This magmatism is preceded by a magmatic event recorded by ~24–20 Ma intrusions located west of the Cauca fault (*Leal-Mejía, 2011*). The Miocene magmatism is documented in the Romeral and Cañas Gordas terranes through 18–6 Ma porphyritic intrusions and volcanic activity. The Mio-Pliocene Combia magmatism is identified within this interval. Combia magmatism was originated by the eastward migration of a Middle-Miocene magmatic belt, which was originally located in the Western Cordillera of Colombia and migrated to the inter-Andean valley. The migration of this magmatism is linked to the Miocene accretion of the Baudó terrane onto northwestern South America (*Duque-Caro, 1990*; *Cediel et al., 2003*). The Combia event is characterized by tholeiitic and calc-alkaline geochemical signatures, which relate its volcanic and intrusive rocks to a magmatic arc extended in part of the northern Andes (*Marriner and Millward, 1984*; *Leal-Mejía, 2011*; *Borrero and Toro-Toro, 2016*). The Combia event is allegedly linked to the activity of the Cauca-Romeral fault system, which may have favored the emplacement of hypabyssal intrusions in the inter-Andean valley (*López et al., 2006*).

The end of the Miocene magmatism in the Central and Western Cordilleras of Colombia lead to the recent magmatism of Colombia, that includes active volcanic complexes in the south and central regions of Colombia (*Marriner and Millward, 1984*). Although this magmatism started ~3 Ma ago, and it is identified by changes in the geochemical signature (*Marriner and Millward, 1984*; *Leal-Mejía, 2011*), its earliest eruptive episodes may be attributed to the 6 Ma Irra Formation (*Toro et al., 1999*); however, a genetic relationship between the Irra and younger events has not been demonstrated.

3. LOCAL GEOLOGY

The Amagá basin is located in a tectonic mélange area with a confluence of rocks of oceanic affinity, low-grade metamorphic rocks, and Triassic igneous rocks (*Sierra and Marín-Cerón, 2011*). The rocks of oceanic affinity in the study area (central part of the Amagá basin) are known as the Cretaceous Quebradagrande Complex (*Calle et al., 1980*; *González, 2001*). The Quebradagrande Complex is in fault contact with low-grade metamorphic rocks whose origin, lithostratigraphy and age have not been clearly established. The metamorphic rocks are mapped as the Paleozoic-Jurassic (?) Cajamarca Complex (*Calle et al., 1980*; *Maya and González, 1995*; *Blanco-Quintero, 2014*). In fault contact with the low-grade metamorphic rocks, there are Triassic igneous rocks called Pueblito Diorite, Romeral Gabbros and Ultramafic Rocks (Fig. 2) (*González, 2001*; *Rodriguez-Jimenez, 2010*).

The sedimentary infill of the Amagá consists of terrigenous strata of the Amagá Formation; this unit is characterized by Oligocene-Miocene continental deposits (*Grosse, 1926*; *Van der Hammen, 1960*; *Silva et al., 2008*; *Sierra and Marín-Cerón, 2011*). Discordantly, Mio-Pliocene volcaniclastic rocks of the Combia Formation overlie the Amagá Formation. The Combia event also contains Mio-Pliocene hypabyssal rocks, which intruded the Amagá Formation between ~10 and ~7 Ma (*MacDonald, 1980*; *Restrepo et al., 1981*; *González, 2010*; *Leal-Mejía, 2011*). The hypabyssal rocks of the Combia event are divided into lithological units that are distinct from the volcano-sedimentary rocks of Combia Formation. *Grosse (1926)* divided these hypabyssal intrusives into various types of basalts and andesites based on their composition, and *Calle et al. (1980)* divided these rocks into basaltic dykes and sills, andesitic dykes and sills, and porphyritic hypabyssal rocks. The available geological maps of the Amagá basin do not make a clear distinction between sills, dykes, or stocks for these rocks.

The structural geology of the central Amagá basin is dominated by a series of NNW-SSE-trending faults belonging to the Cauca-Romeral fault system. Emplacement of the hypabyssal intrusives of the Combia event was partly controlled by these faults, as suggested by the elongation of some intrusives in a NNW direction (Fig. 2). The most important local fault is the Sabanalarga fault, which has a notable geomorphic expression with an elevation drop of over 1300 m across the fault. This fault, which has been referred to as the East Cauca fault (*Grosse, 1926*), juxtaposes low-grade metamorphic rocks against rocks of oceanic affinity and Oligocene-Miocene sedimentary rocks (*Grosse, 1926*). *Calle and González (1980)* reported post-Pliocene activity in the Sabanalarga fault based on field relations. Also important in the central Amagá basin is the Quirimará fault, which is a reverse fault that juxtaposes low-grade metamorphic rocks of the Cajamarca Complex with sedimentary rocks of the Amagá Formation (*Grosse, 1926*). The eastern part of the study area is crossed by the north-trending Cascajosa fault, which is a normal fault that affects Triassic igneous rocks and Oligocene-Miocene sediments (Fig. 2) (*Grosse, 1926*; *Calle and González, 1980*; *Murillo, 1998*). The fault geometry described by these three structures is cinematically incompatible, with near parallel normal, right lateral, and inverse faults; this suggests that at least two deformation events have affected the basin. Major faults usually do not cut hypabyssal rocks of the Combia event, but field evidence suggests that they are affected by minor faults (*Calle and González, 1980*).

4. SAMPLING AND METHODOLOGY

This study presents field work and morphotectonic analysis, petrography, rock magnetic, anisotropy of magnetic susceptibility (AMS), and paleomagnetic data for hypabyssal intrusive bodies of the Combia event in the central part of the Amagá basin. We sampled sixteen outcrops in nine intrusive bodies of the Combia event (Fig. 2).

We carried out a morphotectonic analysis of the study area with the goal of determining the structure and geometry of the hypabyssal rocks of the Combia event, and their relationship with the host rock. This study was performed using aerial images of the study area and the results were verified by field work. We identified planar features associated with sills. Well-developed dip-slopes allow us to solve the three-point problem to determine the attitude of a slope-plane that can be then compared with the attitude of the host rock (and the attitude of the magnetic foliation shown below).

For sample petrography, we used an Olympus BX43 binocular microscope in ten thin-sections, which provided compositional and textural data that were used to determine the effects of the local faults on the hypabyssal rocks of the Combia event. Another step involved characterizing the groups of minerals carrying magnetization and their magnetic susceptibility; this involved hysteresis measurements using a Micromag AGM 2900 from Princeton Instruments. The hysteresis cycles were measured in rock fragments weighing 0.25 to 0.5 mg by applying a saturation field (B_{sat}) of 1 T. We also obtained isothermal remanent magnetization acquisition curves (*IRM*) using the same equipment. For the paleomagnetism and anisotropy of magnetic susceptibility (AMS) studies, between six and twelve rock cores were collected from the intrusive hypabyssal rocks of the Combia event. These cores were extracted using a portable drilling machine and using a solar and a magnetic compass for orientation. The cores had diameters of 2.5 cm and were cut to lengths of 2.1 cm.

The first phase of laboratory analysis consisted of AMS measurements, using a Kappabridge AGICO KLY-3. This equipment was used to determine the principal axes of the susceptibility tensor based on 15 directions (*Jelínek, 1977*). The results were processed through Anisoft 4.2 software (*Chadima and Jelínek, 2009*). The second phase consisted of measuring the natural remanent magnetization and determining its vectorial composition; in this phase, the samples were subjected to progressive demagnetization in alternating fields (3, 6, 9, 12, 16, 20, 25, 30, 35, 40, 50, 60, 70, 80 and 90 mT) using an AGICO LDA-3A device. Samples were measured in an AGICO JR5 spinner magnetometer. The vectorial composition of the natural remanent magnetization (*NRM*) was analyzed via inspection of orthogonal demagnetization diagrams (*Zijderveld, 1967*), and the directions were calculated using the method of principal components (*Kirschvink, 1980*). After determining the directions of the magnetic components of each specimen, *Fisher (1953)* statistical calculations were conducted to determine the mean declination and inclination of each site and estimate the dispersion and confidence cone. All of the measurements were performed in the Laboratorio de Paleomagnetismo del Centro de Geociencias CGEO (UNAM-Campus Juriquilla).

5. RESULTS

5.1. Field relationship and morphotectonic analyses

Our observations of aerial images and the field work show that some of the intrusives are planar in shape, and usually have semi-parallel contacts with the layers of the host rock (they can be recognized as sills). On the other hand, other intrusive rocks form prominent cylindrical elevations and have been interpreted as stocks (Table 1). An even smaller number of bodies may be sub-volcanic as they are annular in shape. Some bodies belonging to the Combia event are cut by minor faults, which correspond to previously mapped faults in the study area. Larger intrusions terminate against large faults, such as the Corcovado Andesite (Fig. 2). We did not observe within the igneous rocks, features such as magmatic foliation, or any other macroscopic fabric, that could be related with motion on these faults.

The relationship between deformation and intrusion is unclear, as some of the intrusive bodies are concordant and others discordant with bedding in Amagá strata. Nonetheless, most authors suggest that the hypabyssal rocks do not record the same intensity of deformation than the Amagá Formation (*Grosse, 1926*). For the sills, for example, it is unclear if they were intruded horizontal (as most sills do) and then tilted, or they must be considered in in-situ coordinates as *MacDonald (1980)* did, for instance, for the Corcovado Andesite.

The bodies located west of the Sabanalarga fault correspond to the sites Ts12, Ts14, Ts15, Ts16, Ts17, Ts18, Ts19, Ts20, Ts21, Ts22 and Ts23. The intrusion at site Ts12 has a planar shape, and an approximate outcrop length of 3.5 km. *Grosse (1926)* describes this body as a sill, however, we cannot observe the contact between the host rock and the hypabyssal rock in this site. This body intrudes layers of the Amagá Formation, which in this area has an attitude of 355/60 (strike/dip). Another body with morphology parallel to the layers of the host rock corresponds to the intrusion sampled at sites Ts16, Ts17 and Ts21; these sites belong to a body with an outcrop length of about 400 m, which intrudes layers with attitude of 70/40 in the western sector of the body and 355/60 in the east part of the body. The outcrop pattern and aerial images, however, suggest that the body at site Ts12 may be the southern continuation of the intrusive sampled at Ts16, Ts17 and Ts21 (Fig. 3). In the foothills east of Bolombolo (Fig. 2) we sampled two stocks with different morphologies. Site Ts15 corresponds to a stock elongated towards the NE; this body has approximate length of 1.75 km and 250 m of width, and it intrudes layers with an attitude of 009/50. Another stock corresponds to the sites Ts14, Ts18, Ts19, Ts20, Ts22 and Ts23. This body has an elliptical cross section with a width of ~650 m and a maximum length of 1.1 km, and intrudes layers with NNW strikes and intermediate dips to the east. We refer to this body as the Bolombolo stock.

The southern area, between Sabanalarga and Cascajosa faults, is characterized by planar bodies with semi-parallel morphologies to the layers of the Amagá Formation; they are thus interpreted as sills (Fig. 3). The intrusive body at site Ts10 is a sill with an approximate length of 2.5 km; this body intrudes layers of the Amagá Formation with NE strike. Another sill can be observed at site Ts11; this sill has an approximate length of 1.4 km, and it intrudes sedimentary layers with NE strike and dip of about 30°.

Table 1. Anisotropy of magnetic susceptibility data of hypabyssal rocks of the Combia event. n: number of specimens measured, K_m: mean magnetic susceptibility, P_j: anisotropy degree, T: shape parameter, K_1, K_2 and K_3: directions of maximum, intermediate and minimum susceptibility, D: declination, I: inclination, $\alpha_{95}(\cdot)$: corresponding 95% confidence angles. Statistics after *Jelínk (1981)*.

Site	Rock	Body	n	K_m [10^{-2}]	P_j	T	K_1				K_2				K_3			
							D [°]	I [°]	$\alpha_{95}(D)$ [°]	$\alpha_{95}(I)$ [°]	D [°]	I [°]	$\alpha_{95}(D)$ [°]	$\alpha_{95}(I)$ [°]	D [°]	I [°]	$\alpha_{95}(D)$ [°]	$\alpha_{95}(I)$ [°]
Ts10	Porhpyr. Andesite	Sill	8	31.1	1.027	0.378	77.4	3.9	13.3	7.0	168.1	9.3	19.2	10.9	324.9	79.9	17.8	6.9
Ts11	Porhpyr. Basalt	Sill	12	16.8	1.073	–0.309	102.0	31.2	9.9	4.5	210.3	27.3	24.6	9.4	332.8	46.2	24.6	3.0
Ts12	Diabase	Sill	11	50.1	1.012	–0.458	106.9	25.7	9.9	5.5	13.8	6.4	22.8	6.6	270.9	63.4	23.5	6.8
Ts14	Diabase	Stock	11	49.9	1.025	–0.186	287.9	27.7	28.7	9.1	189.3	15.9	25.1	12.8	72.9	57.3	25.7	20.3
Ts15	Diorite	Stock	8	45.8	1.009	0.356	38.1	37.4	17.6	9.7	197.4	50.8	21.4	14.5	300.2	10.2	20.4	6.0
Ts16	Porhpyr. Basalt	Sill	13	63.3	1.044	–0.305	157.6	43.0	10.7	4.8	248.4	0.8	14.7	10.1	339.3	47.0	14.5	5.5
Ts17	Porhpyr. Basalt	Sill	13	53.5	1.035	0.453	261.3	40.7	41.2	10.3	151.5	21.6	42.3	27.7	40.9	41.6	31.2	7.7
Ts18	Diabase	Stock	14	57.2	1.015	0.165	257.3	12.9	8.1	3.5	164.3	12.7	8.7	3.4	31.2	71.7	4.7	3.6
Ts19	Diabase	Stock	12	45.4	1.014	–0.155	28.9	2.7	16.6	3.6	119.3	8.6	18.5	11.4	281.3	81.0	14.6	4.3
Ts20	Diabase	Stock	9	33.2	1.020	–0.125	15.8	11.9	6.0	3.6	108.4	11.8	22.6	4.2	241.9	73.1	22.3	3.8
Ts21	Porhpyr. Basalt	Sill	17	50.1	1.037	0.050	202.0	10.9	19.4	12.4	296.4	21.7	19.9	13.1	87.0	65.4	16.3	13.5
Ts22	Diabase	Stock	19	121.0	1.011	–0.120	343.3	11.1	23.2	10.9	112.9	72.9	61.2	19.7	250.7	12.9	61.1	11.7
Ts23	Diabase	Stock	14	43.0	1.007	–0.322	127.8	29.4	11.0	6.2	266.0	52.9	36.3	9.7	25.6	20.5	36.3	7.6
Ts24	Porhpyr. Andesite	Sill	11	2.52	1.090	–0.038	63.3	9.5	22.3	11.4	156.1	16.7	21.9	12.4	304.7	70.6	22.9	19.3
Ts26	Porhpyr. Andesite	Stock	9	0.908	1.019	–0.285	303.7	43.3	16.0	5.4	197.2	16.8	53.6	14.7	91.4	41.9	53.6	7.6
Ts27	Porhpyr. Andesite	Stock	8	5.75	1.034	–0.576	231.2	32.1	15.5	8.5	120.8	29.0	41.1	12.4	358.5	44.0	41.2	10.4

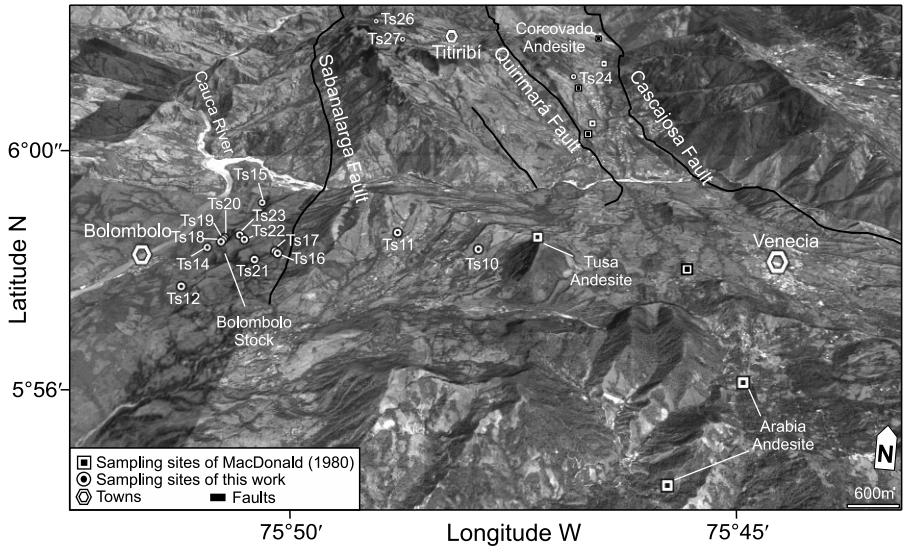

Fig. 3. Oblique aerial view of the study area with sampling sites and dip-slopes to the southeast. Dip-slopes are formed by the contrast between the erosion resistant sills and the friable Amagá strata. The escarpment on the lower left is associated with the Sabanalarga fault.

The northern area between Sabanalarga and Cascajosa faults is crossed by the Quirimará fault. We sampled at three sites in these area (Fig. 2). The body at site Ts24 corresponds to a concordant structure where the bedding of the host rock is 355/45. This intrusive was classified as a sill, and it has a length of 9.25 km; this sill is the Corcovado andesite also sampled by *MacDonald (1980)*. The remaining sites (Ts26 and Ts27) are from two stocks with no clearly defined morphologies (Fig. 2). The bodies at sites Ts26 and Ts27 intrude sedimentary layers with NNW strikes and intermediate inclinations to the east.

The aerial images show evident dip-slopes associated with intrusives interpreted as sills (Fig. 3). For instance, Ts10 and Ts11 were collected in sills forming well-developed planes tilted about 15° to the SE (Fig. 3). The attitude of this plane, determined using the three-point method, compares very well with the attitude of Amagá strata (Table 2). We also calculated the dip-slope attitude at sites Ts12, Ts16 and Ts24. At sites Ts12 and Ts16, we obtained a dip-slope attitude of 25/10 (strike/dip), whilst at site Ts24 the dip-slope attitude is 19/17. Contrary to what was reported by *MacDonald (1980)*, the rotations about horizontal axis are relatively coherent, with moderate tilts to the ESE or SE. Dip-slopes dip, generally, have lower angles than Amagá strata.

5.2. Petrography

The petrography of the hypabyssal rocks of the Combia event showed textural and compositional variations between the different bodies belonging to the rocks of the Combia event (*Tejada et al., unpublished results*). The intrusive bodies at sites Ts10, Ts24, Ts26 and Ts27 are mapped as porphyritic andesites (*Grosse, 1926*; *Calle et al.,*

1980); our field and petrographic observations agree with this classification. The sites Ts10 and Ts24 are characterized by its porphyritic hipocrystalline texture; these rocks are composed of subhedral plagioclase and amphibole phenocrysts embedded in a fine-grained matrix of plagioclase, palagonite, and muscovite with accessories like zircon and opaque minerals. The opaque minerals in these sites are anhedral to subhedral crystals with similar grain size than the matrix (Fig. 4a,b). The sills of the sites Ts11 and Ts16, Ts17 and Ts21 are porphyritic basalts composed of euhedral pyroxene phenocrysts, which are replacing anhedral phenocrysts of amphiboles; these are embedded in a matrix of plagioclase and clay minerals (Fig. 4c,d). The opaque minerals in these sites are anhedral to subhedral crystals embedded in the matrix (Fig. 4c,d). The body at site Ts12 and the Bolombolo stock (sites Ts14, Ts18, Ts19, Ts20, Ts22 and Ts23) have mafic composition (*Grosse, 1926*; *Calle et al., 1980*). The Bolombolo stock is classified as a diabase based on its doleritic texture, with plagioclases interspersed between pyroxene crystals and accessories such as apatite and opaque minerals. The opaque minerals appear like anhedral to subhedral crystals embedded between plagioclases and pyroxenes (Fig. 4e,f). The Site Ts15 presents an important variation contrasting with the other samples. This body is classificated as a diorite, due to its phaneritic texture and mineralogy. This predominantly consists of pyroxene and plagioclase crystals, which are in contact with subhedral to euhedral opaque minerals (Fig. 4g,h). The textural variation in this site regard to the other bodies, suggests that it can be correlated with dioritic bodies from the Combia event located near the town of Titiribí (Fig. 2) (*Uribe-Mogollón, 2013*).

We did not observe ductile or fragile deformational features in any of the rocks; therefore, we infer that the textural and compositional characteristics of the hypabyssal rocks of the Combia event are result of magmatic flow and rock cooling. It is also important to mention that due to the relationships between the opaque minerals and the matrix of the different rocks, we conclude that these minerals are product of the primary crystallization of the rocks. There are no indications of hydrothermal or other type of alteration.

5.3. Magnetic mineralogy

The *IRM* acquisition curves (Fig. 5a) show that magnetic saturation occurs in fields of approximately 150 mT. Site Ts10 reaches a magnetic saturation at a slightly higher field, and only Ts11 continues to acquire a small remanence at inductions above 0.4 T without reaching saturation. Sites Ts21 and Ts22 exhibit somewhat erratic behavior in the acquisition of *IRM*; however, stable paleomagnetic behavior was obtained for site Ts22. This suggests that the erratic behavior in this sample may be an instrumental issue (Fig. 5b). The *IRM* curves indicate components of low coercivity, which are most likely a cubic phase (s) whose magnetic saturation develops in inductions of approximately 150 mT (*Ribeiro et al., 2015*).

The hysteresis cycles yielded typical parameters of the pseudo-single-domain (PSD) field (*Tauxe et al., 2002*; *Dunlop, 2002*). The samples are characterized by remanent saturation magnetization (M_{rs}) values ranging from 34.81 to 316.8 $\mathrm{mAm^2\,kg^{-1}}$ and saturation magnetization (M_s) values ranging from 567.9 to 4933 $\mathrm{mAm^2\,kg^{-1}}$. The remanent coercive force (B_{cr}) and the coercive force (B_c) range from 6.53 to 29.76 mT

Table 2. Paleomagnetic data of hypabyssal rocks of the Combia event. *D*: magnetic declination, *I*: magnetic inclination, α_{95}: 95% confidence interval, *k*: precision parameter of the Fisher distribution (*Fisher, 1953*), *n*: number of specimens measured. Sites marked with (w) are located west of the Sabanalarga fault, the remaining sites are located between the Sabanalarga and Cascajosa faults.

Site		In-Situ					Titl-Corrected				AMS Foliation				Dip-Slope Corrected				Final	
		D [°]	*I* [°]	α_{95} [°]	*k*	*n*	Strike	Dip	*D* [°]	*I* [°]	Strike	Dip	*D* [°]	*I* [°]	Strike	Dip	*D* [°]	*I* [°]	*D* [°]	*I* [°]
Ts10	Sill	10.3	3.5	12.7	94.79	3	60	15	11.9	14.8	54.0	10.0	11.2	10.4	38	15	11.9	10.3	11.7	11.0
Ts11	Sill	347.9	–14.3	3.1	461.14	6	35	30	346.8	8.1	62.0	44.0	349.5	28.0	38	15	346.5	–2.6	347.7	12.4
Ts12(w)	Sill	192.5	14.5	6.6	104.28	6	355	60	170.6	22.2	1.0	27.0	184.5	18.1	25	10	190.2	12.1	188.0	13.6
Ts14(w)	Stock	200.4	–10.6	10.9	50.31	5	355	60	197.6	15.9	166.0	33.0	190.3	–27.2					200.4	–10.6
Ts15(w)	Stock	168.9	36.1	16.8	30.85	4	9	50	149.3	9.6	30.0	80.0	162.2	–24.9					149.3	9.6
Ts16(w)	Sill	24.8	–15.7	5.6	145.36	6	355	60	355.3	–33.3	70.0	43.0	24.8	15.5	25	10	22.0	–15.4	19.3	–18.6
Ts20(w)	Stock	211.1	44.0	10.2	57.36	5	355	60*	141.2	45.6	332.0	17.0	198.3	57.6						
Ts22(w)	Stock	196.4	42.0	3.4	391.25	6	355	60*	142.3	34.7	341.0	78.0	118.0	34.1						
Ts23(w)	Stock	218.7	40.6	15.6	63.52	3	355	60*	146.2	51.2	116.0	70.0	216.9	–28.3						
Ts24	Sill	341.4	4.2	6.7	132.14	5	355	45	348.3	12.6	35.0	20.0	344.1	20.1	19	17	343.6	14.4	343.8	16.8
Ts26	Stock	334.9	18.1	17.5	50.85	4	355	30	346.9	25.6	181.4	48.1	330.2	–6.2	49	11	336.3	28.6	334.9	18.1
Ts27	Stock	334.0	38.4	19.7	40.2	3	350	45	10.8	36.3	88.5	46.0	277.0	70.8	49	11	337.0	49.0	334.0	38.4
Mean		4.4	–12.1	19.5	5.9	12			348.4	–10.2			355.3	11.1						
									$k = 5.9$, $\alpha_{95} = 19.6°$				$k = 3.7$, $\alpha_{95} = 26.4°$							
Selected		357.9	–0.8	19.6	7.8	9			355.0	1.9			354.5	20.2			356.5	10.5	354.8	7.8
									$k = 8.7$, $\alpha_{95} = 18.5°$				$k = 6.2$, $\alpha_{95} = 22.5°$				$n = 7$ $k = 8.0$, $\alpha_{95} = 22.8°$		$n = 9$ $k = 9.2$, $\alpha_{95} = 17.9°$	

Table 2. Continuation, data of *MacDonald (1980)*

Site		In-Situ					Titl-Corrected				AMS Foliation				Dip-Slope Corrected				Final	
		D [°]	I [°]	α_{95} [°]	k	n	Strike	Dip	D [°]	I [°]	Strike	Dip	D [°]	I [°]	Strike	Dip	D [°]	I [°]	D [°]	I [°]
C1	Sill	325.0	–14.9	3.1	610	5	355	45	323.0	9.2	35	20	324.3	4.0	19	17	323.6	–1.0	320.0	1.1
C2	Sill	320.5	8.4	14.3	66	3	355	45	343.3	23.2	35	20	333.4	26.3	19	17	333.6	20.9	333.4	23.2
C3	Sill	320.9	10.8	3.3	1409	3	355	45	337.5	31.5	35	20	323.1	29.9	19	17	323.9	25.0	323.6	27.1
C4	Sill	320.1	–7.6	9.9	644	2	355	45	323.7	17.9	35	20	320.3	11.7	19	17	320.1	7.0	320.2	9.0
P18	Sill	336.4	4.9	3.5	142	13	355	45	345.1	16.6	35	20	339.0	21.8	19	17	338.8	16.2	338.9	18.6
C11	Stock	305.2	–22.8	5.5	192	5					54	10	306.2	–13.3	38	15	305.4	–7.8	305.9	–10.0
C12	Stock	335.9	–23.0	3.7	222	8					54	10	335.2	–13.2	38	15	333.9	–9.6	334.6	–10.7
C8	Stock	304.7	53.9	4.3	312	5									310	39	348.5	41.5	348.5	41.5
C9	Stock	322.4	60.0	2.3	1125	5									310	39	2.2	37.3	2.2	37.3
Mean		346.5	–4.1	16.9	4.5	21			344.0	–0.5			342.9	10.9						
									$n = 17$ $k = 6.34$, $\alpha_{95} = 15.4°$				$n = 19$ $k = 4.64$, $\alpha_{95} = 17.5°$							
Selected		340.9	3.1	15.8	5.7	18			347.5	8.8			341.0	15.9			342.0	13.3	342.8	12.1
									$n = 14$ $k = 9.6$, $\alpha_{95} = 13.6°$				$n = 16$ $k = 7.0$, $\alpha_{95} = 15.1°$				$n = 16$ $k = 8.34$, $\alpha_{95} = 13.6°$		$n = 18$ $k = 8.6$, $\alpha_{95} = 12.5°$	

and from 2.775 to 13.36 mT, respectively. The B_{cr}/B_c ratio ranges from 2.116 to 4.471, and the M_{rs}/M_s ratio ranges from 0.037 to 0.120. Both ratios are plotted on the diagram after *Dunlop (2002)*. The specimens plot in the PSD field, where mixing lines of multi-domain (MD) and single-domain (SD) particles plot as well (Fig. 5b). The *IRM*s suggest that a hard phase such as hematite or goethite is not present (except for Ts11, but the contribution is in any case small), therefore the magnetization is most likely controlled by

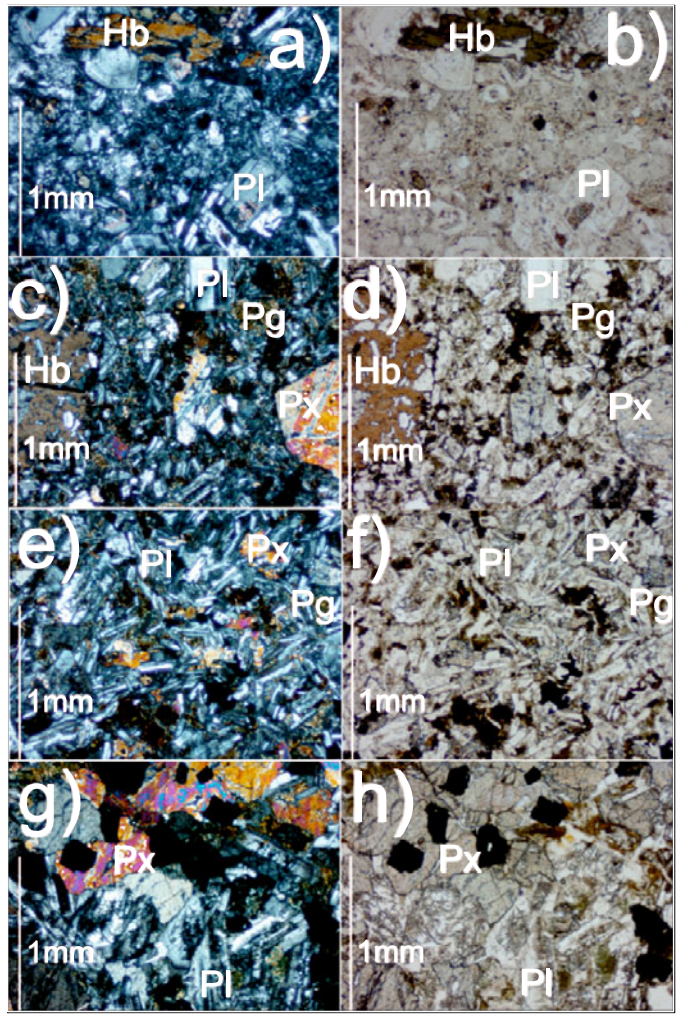

Fig. 4. Petrography of rocks belonging to the hypabyssal rocks of the Combia event. The microphotographs are shown on the left side with crossed nicols and on the right side with parallel nicols. **a, b)** Porphyritic andesite of site Ts10; **c, d)** Porphyritic basalt of site Ts11; **e, f)** Diabase of site Ts14; **g, h)** Diorite of site Ts15. Hb: Hornblende, Pg: Palagonite, Pl: Plagioclase, Px: Pyroxene.

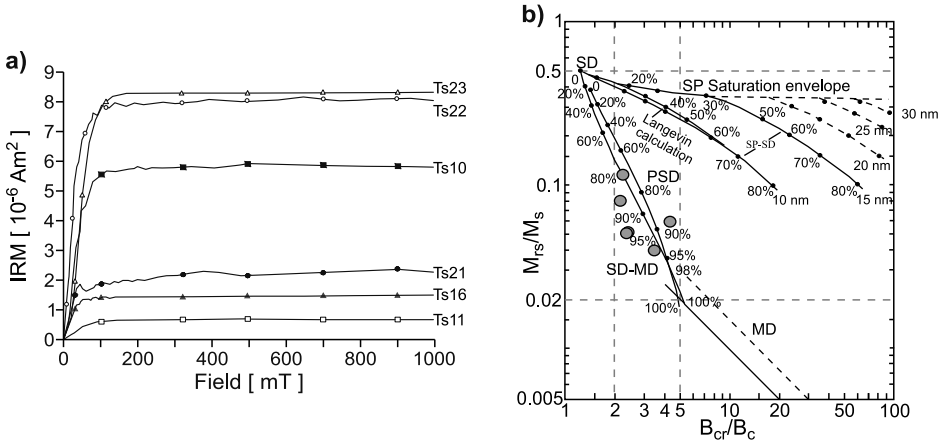

Fig. 5. **a)** Isothermal remanent magnetization (*IRM*) acquisition curves of selected samples of intrusive rocks of the Combia event. **b)** Plot of ratio of saturation remanent magnetization (M_{rs}) to saturation magnetization (M_s) vs. ratio of coercivity of remanenc (B_{cr}) to coercive force (B_c) (*Dunlop, 2002*) of selected samples of intrusive rocks of the Combia event. SP: super-paramagnetic, SD: single-domain, PSD: pseudo-single-domain, MD: multi-domain.

a cubic phase. Results from demagnetization experiments and the range of coercivities observed in hysteresis curves support this interpretation (*Peters and Dekkers, 2003*). The limited observations of oxides in thin sections suggest that the cubic phase is magnetite or titanomagnetite.

5.4. Anisotropy of magnetic susceptibility

We obtained magnetic fabric data for 16 sites where hypabyssal intrusive rocks of the Combia event are exposed (Table 1). The intensity of the preferred orientation of the minerals which control the low field susceptibility in the intrusive rocks is indicated by the anisotropy degree P_j. The rocks of the Combia event have low values of P_j ranging from 1.007 to 1.090, and values of mean magnetic susceptibility K_m between 0.908×10^{-3} and 121×10^{-3} (SI units, Table 1). The relationship between K_m and P_j shows ferromagnetic contributions to the magnetic fabrics of the hypabyssal rocks of the Combia event, with K_m values higher than 10^{-3} in almost all sites (Table 1; Fig. 6a) (*Rochette, 1987*; *Rochette et al., 1992*). Only at site Ts26 the fabric may have paramagnetic contributions to the magnetic fabric, with a K_m value of 0.908×10^{-3}.

The susceptibility ellipsoid is characterized by the shape parameter T, where $T < 0$ denotes prolate ellipsoids, and $T > 0$ denotes oblate ellipsoids (*Jelínek, 1981*; *Hrouda, 1982*). Based on this criterion, sites Ts10, Ts15, Ts17 and Ts18 have oblate fabrics, and sites Ts11, Ts12, Ts14, Ts16, Ts19, Ts20, Ts22, Ts23, Ts26 and Ts27 have prolate fabrics. The remaining sites, Ts21 and Ts24 have triaxial fabrics, which are indicated by T values close to 0 (Fig. 6b).

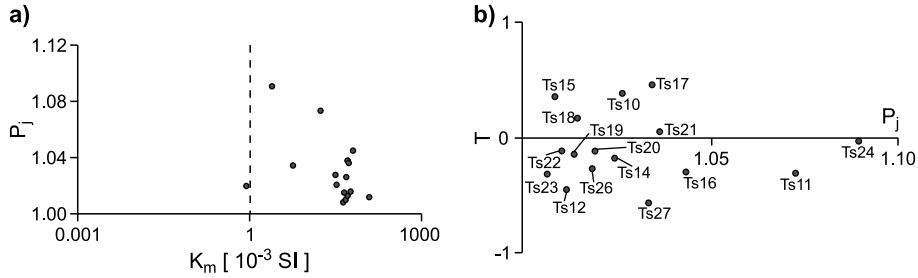

Fig. 6. Plots of magnetic anisotropy parameters. **a)** Anisotropy degree P_j vs. mean magnetic susceptibility K_m, **b)** shape factor T vs. P_j.

In intrusive hypabyssal rocks, such as sills of intermediate to basic composition, the magnetic foliation is expected to be perpendicular to maximum compressive stress σ_1, and in a horizontal sill this direction is expected to be near vertical (K_3 normal to the intrusion plane), even when the flow velocity controls the fabric (*Tarling and Hrouda, 1993*; *Dragoni et al., 1997*; *Rochette et al., 1999*; *Liss et al., 2002*). Weakly oblate fabrics with subhorizontal foliation are expected under moderate magma velocity conditions, and prolate fabrics at greater velocity. Magnetic lineation is generally controlled by the velocity of magma flow, producing either flow parallel maximum susceptibility or gentle imbrication of the magnetic foliation plane (*Tarling and Hrouda, 1993*).

The assumption of a K_3 normal to the intrusion plane is apparently observed in the southern area between Sabanalarga and Cascajosa faults. The sites Ts10 and Ts11 have subvertical K_3 and shallow dipping magnetic foliation planes with inclinations to the southeast. These planes are concordant with the bedding of the Amagá Formation in both sites (Fig. 7). Dip-slopes developed over these erosion-resistant units are tilted about 15° to the southeast (Fig. 3), which compare well with the magnetic foliation and the attitude of Amagá strata (Table 2).

The northern area between the Sabanalarga and Cascajosa faults is well illustrated by the site Ts24, which has a nearly vertical K_3 that defines a magnetic foliation plane slightly dipping to the southeast; however, the magnetic foliation is oblique to the 45° eastward dip of the Amagá Formation. The Corcovado andesite is a sill with a well developed dip-slope dips about 17° to the ESE, which compares well with the magnetic foliation plane (strike 35°, dip 20°), but not so with the attitude of Amagá strata (Table 2). In this site, the magnetic foliation is nearly parallel to the NE-SW contact between the hypabyssal intrusive and the host rock (Fig. 7). It thus appears that magnetic foliation may provide a good estimate of paleo-horizontal when bodies are planar.

Other intrusions sampled in the northern area between Sabanalarga and Cascajosa faults are the stocks at sites Ts26 and Ts27. They intruded layers of the Amagá Formation with NNW strike and dips between 30° and 45°. The magnetic foliation plane at site Ts26 is dipping to the west and has N-S strike; the magnetic lineation at this site is oriented towards NW. On the other hand, at site Ts27, the magnetic foliation has a E-W strike with an intermediate dip towards the south; the magnetic lineation at this site has a SW strike (Fig. 7).

West of the Sabanalarga fault, we sampled the sill at site Ts12 and its northern continuation at sites Ts16, Ts17 and Ts21. The site Ts12 has a magnetic foliation plane sub-parallel to the attitude 355/60 of the host rock (Fig. 7); a dip-plane was also determined for site Ts12; it agrees well with the magnetic foliation but not so with the attitude 355/60 of the host rock (Table 2). The northern continuation of this body does not have a clear relationship between the host rock bedding and the magnetic foliation plane. The sites Ts17 and Ts21 have southwest to west moderately dipping magnetic foliation planes, whilst the site Ts16 has a magnetic foliation which dips towards the south. At sites Ts16 and Ts17, the sill intrudes layers of the Amagá Formation with an attitude of 355/60. Both sites do not present concordance between their magnetic foliation planes and the attitude of the layers of the host rock. The site Ts21, which also belongs to this sill, has a contact of attitude 70/40 with the host rock. The magnetic foliation at this site is oblique

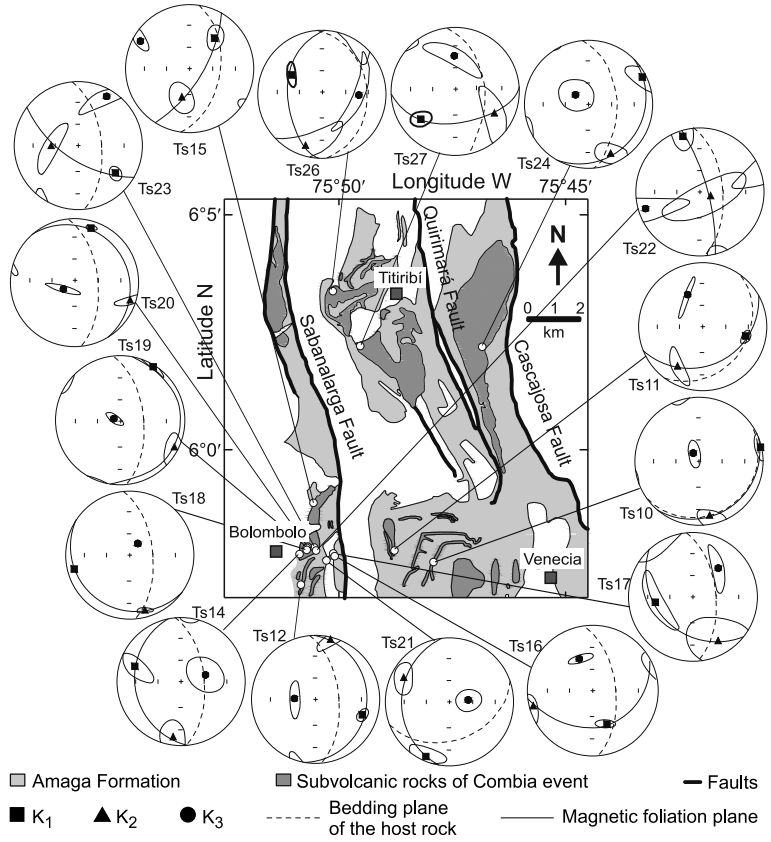

Fig. 7. Stereographic projections of magnetic fabric data of intrusive rocks of the Combia event. The principal susceptibility axes (maximum K_1, intermediate K_2 and minimum K_3) are shown along with their confidence angles. All projections are in the lower hemisphere. The strike and dip of the host rock (Amagá Formation) also is showed. Confidence intervals after *Jelínek (1981)*.

to the bedding of the Amagá Formation (Fig. 7). These sites are in foothills near the trace of the Sabanalarga fault.

West of the Sabanalarga fault there are AMS data for two stocks. The stock at site Ts15 has a subvertical magnetic foliation plane with NE-SW orientation; this plane is oblique to the bedding 009/50 of the layers of the Amagá Formation. The fabric at this site is considered as a magnetic fabric controlled by magmatic flow due to the northeast trends of the intrusion and its magnetic lineation, as well as the prolate fabric. Another stock located in this area corresponds to the sites Ts14, Ts18, Ts19, Ts20, Ts22 and Ts23, assigned to the Bolombolo stock. At the Bolombolo stock the minimum susceptibility direction deviates slightly from vertical and defines planes that dip at shallow angles towards the west at site Ts14, to southwest at site Ts18, to east at site Ts19, and to northeast at site Ts20. The remaining sites Ts22 and Ts23 have steep foliation planes with dips towards the NE and SW, respectively. The site Ts23 is located in the east margin of the body and it is the only site with apparent concordance between the magnetic foliation plane and the bedding of the Amagá Formation (355/60) (Fig. 7).

5.5. Natural remanent magnetization

A characteristic magnetization (*ChRM*) was determined at 12 sites (Table 2). At the 4 other sites, there was no stable behavior during demagnetization. The specimens generally have a multi-vectorial magnetization. Nonetheless, low coercivity components are easily removed, revealing the *ChRM*, which reaches the origin or shows a good trend to the origin in inductions of 40 to 60 mT (Fig. 8). Some dispersion may be observed in the linear trends to the origin (Fig. 8a), but this is attributed to instrumental noise or acquisition of small anhysteretic magnetizations at high inductions. Low-coercivity components are considered secondary and may be viscous (Fig. 8b), spurious (Fig. 8c) or, occasionally, isothermal magnetizations (induced by lightning, Fig. 8d). These components are erased in low fields of 3 to 6 mT. The *ChRM*s obtained after demagnetization change between NE and NW directions (Fig. 8), although other sites exhibit directions to the SSW (Fig. 8e). All components interpreted as *ChRM*s had maximum angular deviation (*MAD*) values smaller than 15°.

Site-mean directions are relatively well defined. The dispersion is relatively low at each site, with the precision parameter of the *Fisher (1953)* distribution k values greater than 30 (Table 2); however, the dispersion between site-means in both, in-situ and tilt-corrected coordinates (assuming the dip of adjacent strata), is anomalously high ($k \sim 5$). The paleomagnetic directions show five sites with normal polarity as interpreted from northwest to northeast directed magnetizations, four sites have reverse polarity as interpreted from south directed magnetizations, and three sites have intermediate directions, with declinations to the southwest and moderate positive inclinations. The latter group is characterized by sites from the Bolombolo stock. The presence of sites with different polarity supports (although does not prove) the absence of a regional remagnetization event in the study area, and it suggests that sufficient time averaged secular variation (*Van der Voo, 1990*); it also suggests that the *ChRM* is a primary thermoremanent magnetization (*TRM*). A similar conclusion was reached by *MacDonald (1980)*, but no field test was possible due to outcrop quality at intrusive contacts.

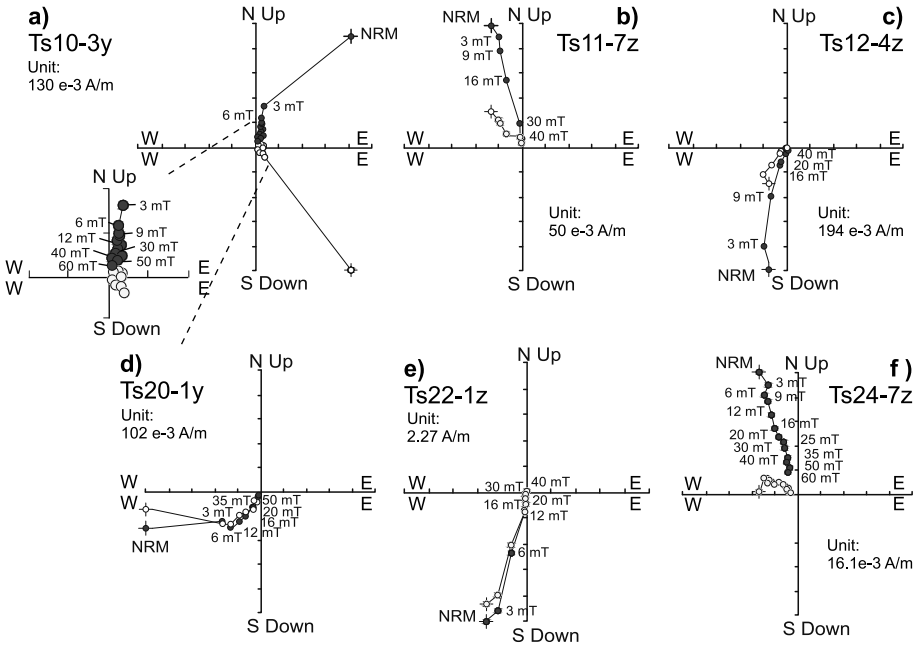

Fig. 8. Orthogonal demagnetization plots (*Zijderveld, 1967*) of selected samples belonging to the hypabyssal rocks the Combia event for sites: **a)** Ts10, **b)** Ts11, **c)** Ts12, **d)** Ts20, **e)** Ts22, **f)** Ts24. Empty circles are projections on a vertical plane and full circles are projections on a horizontal plane.

Considering the in-situ directions (i.e., assuming that the intrusions postdate the deformation of the Amagá Formation, and sills were intruded at moderately dipping angles), we obtained a mean paleomagnetic declination $D = 4.4°$ and inclination $I = -12.1°$ ($\alpha_{95} = 19.5°$, $k = 5.9$) in 12 sites and a mean paleomagnetic direction of $D = 346.5°$, $I = -4.1°$ ($\alpha_{95} = 16.9°$, $k = 4.5$, $n = 18$) including the sampling sites reported by *MacDonald (1980)* (Fig. 9a). The negative mean inclination is not consistent with emplacement in the northern hemisphere. After correcting these directions based on the bedding attitudes of the Amagá Formation, which were measured at locations closest to the sampling sites or at the sites themselves, we obtained a mean paleomagnetic direction of $D = 348.4°$, $I = -10.2°$ ($\alpha_{95} = 19.6°$, $k = 5.9$) in 12 sites and a mean paleomagnetic direction of $D = 344.0°$, $I = -0.5°$ ($\alpha_{95} = 15.4°$, $k = 6.34$, $n = 17$) including the sampling sites of *MacDonald (1980)* (Fig. 9b). Thus, after the structural correction, the values of α_{95} and k do not exhibit significant changes. Based on these data, it appears that the correct reference frame is ambiguous; it is most evident, however, that something additional to secular variation contributes to the high between site dispersion. Possible explanations are tectonic, structural complexity, and/or geomagnetic.

By tectonic explanation we mean there has been relative rotation between sampling localities, coherent or not coherent, about vertical axes. For example, *MacDonald (1980)*

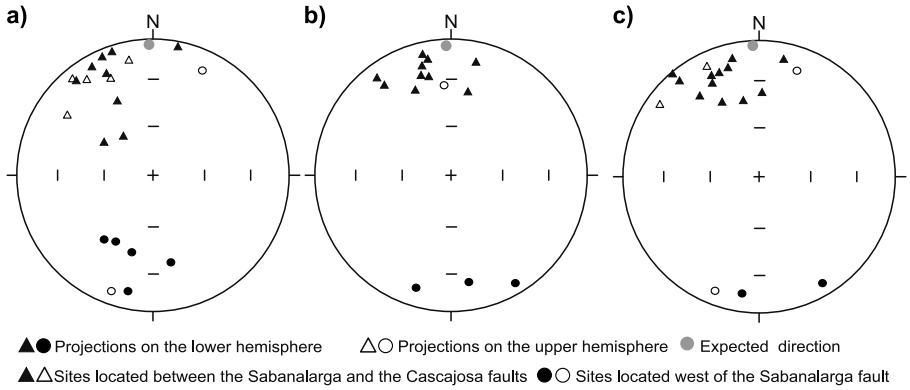

Fig. 9. Stereographic projections of paleomagnetic mean directions including the expected magnetic directions for 10 Ma (*Besse and Courtillot, 2003*). **a)** Paleomagnetic mean directions in the in-situ coordinate system; **b)** paleomagnetic mean directions in the tilt-corrected coordinate system. The sites with transitional directions (Ts20, Ts22 and Ts23) were excluded. **c)** Selected paleomagnetic mean directions.

inferred counterclockwise rotation about a vertical axis for the Corcovado andesite due to tectonic processes. Implicitly in this interpretation, it is the assumption that paleo-secular variation is fully averaged by the five sites collected in this sill. By structural explanations we mean some of the sites require a tilt correction that is not consistent with the tilt of Amagá strata. We notice, for instance, that the tilt of site Ts24 in the Corcovado andesite (dip-slope and magnetic foliation) is at a smaller angle than the dip of Amagá strata. By geomagnetic explanation we mean that there are records of geomagnetic excursions or anomalous field directions.

A geomagnetic explanation is preferred for sites Ts14, Ts20, Ts22 and Ts23, which represent the Bolombolo stock. All four sites show declinations to the SSW and moderate values of magnetic inclinations, which are positive for sites Ts20, Ts22 and Ts23 (and remain positive after a tilt correction assuming the tilt of Amagá strata), and shallow negative for Ts14. Sites with moderate positive inclinations exhibit paleomagnetic directions distinct from the directions observed at the nearest sites, such as Ts12 and Ts16, which have SSW declinations but shallow inclinations. Another site that is close, but no as close as the other sites, is the site Ts15. It has a southeast declination and moderate positive inclination. No single tilt correction brings both, SSW directed shallow negative directions and SSW directed moderate positive directions, to coincide with the expected direction ($D = 357°$, $I = 6.3°$; *Besse and Courtillot, 2003*) or the northwest directed direction recorded in sites such as Ts11, Ts24 and others. Furthermore, most of the sites in the foothills of the Sabanalarga fault are characterized by magnetic foliation planes that dip at shallow angles; this is consistent with an emplacement close to their present attitude (again assuming σ_1 vertical and K_3 near the vertical). A possible interpretation for the anomalous paleomagnetic directions of the sites Ts20, Ts22 and Ts23 is that the paleomagnetic directions at these sites indicate significant deformation or other process such as slumping, but we rule out this explanation because the bedding planes in the

Amagá Formation dip to the east fairly uniformly along the trace of the Sabanalarga fault. Another possible explanation for these anomalous paleomagnetic directions is that sites Ts20, Ts22 and Ts23 might have recorded transitional directions of a magnetic field excursion, and that is our preferred interpretation.

Structural correction

We recalculated the mean paleomagnetic direction excluding the three sites with anomalous directions in in situ and in tilt-corrected coordinates; nevertheless, the improvement of the k and α_{95} values of the mean paleomagnetic direction is marginal (Table 2). The precision parameter increases to values of 7.8 and 8.7 for in situ and tilt-corrected coordinates, respectively. We conclude that even if anomalous field behavior is considered, the high dispersion of site means cannot be yet explained. The dispersion of the nine selected site means, estimated from the angular standard deviation, is greater than expected from secular variation models. We thus consider alternate approaches to tilt correction using AMS data and the attitudes of dip-slope planes as explained below.

The intrusion at site Ts24 was also sampled by *MacDonald (1980)*, and was designated as the Corcovado Andesite. This author reported an in-situ direction similar to that observed at site Ts24, which is to northwest with shallow inclination. The mean of six sites in situ coordinates is $D = 328°$, $I = -1°$. If we apply a tilt correction based on the attitude of the dip-slope, the mean direction of the sites in the Corcovado andesites remains shallow to the northwest ($D = 330.6°$, $I = 13.1°$), but it is closer to the expected direction than *in-situ* or corrected according to the dip of Amagá strata directions. We thus conclude that sills such as Corcovado andesite (Ts24), Ts10, Ts11 and Ts12 require to be restored to the paleo-horizontal, and the AMS or the dip-slope provide a reasonable estimate of the restoration required; in practice we used both. Other units sampled by *MacDonald (1980)* were not sampled in this study, but the sites collected by this author near to the Tusa andesite are at the base of the dip-slope of the sites Ts10 and Ts11 (Fig. 3). The directions observed in the sites at Tusa andesite are to the northwest and of negative inclination, yet correcting according to the magnetic foliation planes, it transforms these directions to the northwest and assigns a positive inclination (closer to the expected direction; Table 2). This exercise suggests, again, that a structural correction is required. The tilt determined for the site Ts10 can thus be used to restores sites collected in the Tusa Andesite.

A structural correction for sites collected in non-planar bodies is not straightforward; a dip-slope cannot be estimated. Magnetic foliation cannot be used to correct at site Ts15, for instance, because the assumption of an originally subvertical k_{min} must be rejected (it would require a tilt greater than indicated by Amagá strata). The approach we took is to compare the observed direction in different coordinate systems with the expected. Using this approach, we conclude that site Ts15 requires a structural correction, and the bedding of adjacent Amagá strata provides the best available correction. In contrast, it appears that site Ts14 does not require a structural correction, or at least not one that can be justified by geological or other observations. A similar conclusion was reached for the stocks collected at Ts26 and Ts27, which are reported in in-situ coordinates.

A morphotectonic analysis allows us to restore sites collected by *MacDonald (1980)* at the La Arabia body, which has *in-situ* directions with anomalous high inclinations (~60°).

Corrected for the attitude of a dip-slope, they yield inclinations of ~40°. We assume that if a tilt corrected paleomagnetic direction lies closer to the expected direction, and the site dispersion decreases, we can provide better estimates of rotation about a vertical axis. If the tilt of Amagá and Combia rocks is related to activity along the Romeral fault system, it is implied that rocks of the Amagá Formation had already experienced some deformation prior to the Combia event, even if the Combia rocks were also affected by a second event or had a syn-deformation emplacement.

The structural correction for our data was thus recalculated using the attitude of the magnetic foliation averaged with dip-slop planes as an indicator of tilt for planar sites, the dip-slope alone for sites where AMS data are not available, and bedding for the intrusion at site Ts15. The mean of the sites collected by us is of $D = 354.8°$, $I = 7.8°$ ($n = 9$, $k = 9.2$, $\alpha_{95} = 17.9°$). If we include the data reported by *MacDonald (1980)*, corrected as described above, we obtain a mean of $D = 342.8°$, $I = 12.1°$ ($n = 18$), the value of α_{95} is 12.5° and k is 8.6 (Fig. 9c). The standard angular deviation of the data set is 27°, once again, higher than expected for this latitude according to secular variation models (*Butler, 1992*). We notice, however, that the inclination is now positive and agrees with emplacement in the northern hemisphere.

Due to the complex structural framework of the study area, we recalculated the mean paleomagnetic directions using selected paleomagnetic directions according to the location of the different sites. We present a mean paleomagnetic direction of $D = 336.6°$, $I = 17.4°$, $\alpha_{95} = 11.7°$, $k = 12.45$ for 14 sites located east of the Sabanalarga fault and west of the Cascajosa fault. This division of the paleomagnetic data reduces α_{95} value and increases the k value. The remaining sites, which are located west of the Sabanalarga fault have a mean paleomagnetic direction of $D = 4.4°$, $I = 1.0°$, $\alpha_{95} = 34.0°$, $k = 8.26$ for 4 sites.

6. DISCUSSION

The Mio-Pliocene tectonic activity in northwestern South America is responsible for the geological framework of the inter-Andean sedimentary basins, including the Amagá basin (*Acosta, 1978*; *Alfonso et al., 1994*; *Sierra, 1994*; *Sierra and Marín-Cerón, 2011*; *Sierra et al., 2012*; *Montes et al., 2015*). The evolution of the rocks of the Combia event may contain a record of the interaction between various tectonic blocks and its relationship with the geological framework of the northwestern South America (*Duque-Caro, 1990*; *Cediel et al., 2003*; *Sierra and Marín-Cerón, 2011*). The hypabyssal intrusions of the Combia event are marked by their compositional variety, which includes porphyritic andesites, porphyritic basalts, diabases and diorites (*Gonzalez, 2001, 2010*; *Tejada et al., unpublished results*; *Uribe-Mogollón, 2013*). The textural and compositional variations among the hypabyssal rocks of the Combia event indicate changes in the magmatic and crystallization conditions in which these rocks formed.

The different types of rocks are not dissimilar in terms of their hysteresis cycles and *IRM* acquisition curves. Therefore, the minerals that control the magnetization and magnetic susceptibility in these rocks are characterized by low coercivity components, which are linked to magnetite or titanomagnetite. The primary origin of these minerals is

reflected by the textural relationships between the opaque minerals and the other minerals presented in the different intrusive bodies. The contribution of a ferromagnetic component to the magnetization of the hypabyssal intrusive rocks of the Combia event is also shown by K_m values higher than 10^{-3}. Only the site Ts26 has a K_m value that may indicate a possible paramagnetic contribution.

During the Combia magmatic event (Late Miocene), the Romeral fault zone had a dextral behavior (*Sierra et al., 2012*) most likely linked to the accretion of terranes onto the northern Andean block (*Duque-Caro, 1990*; *Cediel et al., 2003*). Because of the geodynamic context and the time that the Combia volcanism occurred, one would expect to find deformational features in the intrusives of the Combia event, as is reflected in the elongated morphologies of certain hypabyssal intrusives; some of them are aligned parallel to the fault systems in the study area. However, the petrography of the hypabyssal rocks of the Combia event does not indicate ductile deformational features, or deformational features of other type. AMS data do not reflect high values of P_j, instead, they present typical P_j values of non-deformed intrusive rocks (*Tarling and Hrouda, 1993*). For these reasons, we infer that the magnetic fabrics were dominated by processes that responded to magmatic flow and the emplacement of these rocks.

Previous studies report activity along the Cauca-Romeral fault system in the Oligocene-Miocene (e.g., *Sierra et al., 1994*; *Cediel et al., 2003*; *Sierra et al., 2012*; *Sierra and Marin-Cerón, 2011*). This activity may be related with the different collisional stages of the Panama-Choco block with the northern Andean block. These collisional periods generated different deformational events which affected the inter-Andean valley and the northwestern margin of South America (*Duque-Caro, 1990*; *Cediel et al., 2003*; *Cortes and Angelier, 2005*; *Suter et al., 2008*; *Montes et al., 2012, 2015*). Therefore, the Oligocene-Miocene Amagá Formation (host rock of the Combia intrusives) was deposited during intense periods of activity of the Cauca-Romeral fault system. Deformation of the Combia intrusions is evident from the tilt of sills, and more convincingly from paleomagnetic directions (discussed below). However, the temporality of the deformation of the host rock has not been clearly established. Considering the geodynamic context of northern South America during the deposition of the Amagá Formation (host rock), and the recorded activity of the fault systems that border the Amagá basin (*Cediel et al., 2003*; *Cortes and Angelier, 2005*; *Suter et al., 2008*), it is possible that the Amagá Formation was deformed before the intrusion of the hypabyssal intrusive rocks of the Combia event. In relation with our AMS data, the most conclusive evidence of deformation prior to the intrusion of the hypabyssal rocks of the Combia event is the angular discrepancy between Amagá Formation tilt, magnetic foliation planes and dip-slopes (such as at Corcovado Andesite), or the fact that some intrusions do not appear to require a structural correction (Ts14), but others do (Ts15).

During the late Neogene, the activity of the fault systems that border the Choco and the northern Andean blocks favored the onset of the obduction of the Cañas Gordas terrane over the northwestern part of the north Andean block (*Cediel et al., 2003*). This event may be responsible for rotations and tilting of the hypabyssal rocks of the Combia event (*Cediel et al., 2003*). *MacDonald (1980)* and *MacDonald et al. (1996)* noticed the uniformity among the intrusions between Titiribí, Bolombolo and Venecia towns (central part of the Amagá basin) (Fig. 2), and specifically their counterclockwise rotations of

approximately 35° and local tilting. However, the absence of structural corrections for those paleomagnetic data reduces the reliability of the interpretation because it is based on in-situ directions; it also implies the assumption that the secular variation was averaged at the level of each intrusion. A more thorough analysis, based on 18 site mean directions with structural corrections, yields an overall mean of $D = 342.8°$, $I = 12.1°$, with very high dispersion ($S = 27°$). It thus appears that although in-situ directions should not be used, we still need to consider deformation (relative rotation between localities) as a possible explanation for the dispersion of site means. A likely source of dispersion not related to secular variation is relative rotation between localities about a vertical axis. We calculated the mean of in-situ and tilt-corrected inclinations (*Kono, 1980*). A positive tilt test using the simple test of *McElhinny (1964)* is obtained comparing the statistics of 18 in-situ and 18 tilt-corrected site means ($k_2/k_1 = 2.06$, where k_1 and k_2 are precision parameters before and after tilt correction, respectively). The angular standard deviation of the average inclination is 17.9° (consistent with paleo-secular variation) and the tilt corrected mean inclination is 12.3 ± 10.5.

Although based on a small number of sites (6), the mean of the Corcovado andesite *ChRM* is well defined yielding a mean of $D = 330.6°$, $I = 16.2°$, $\alpha_{95} = 11°$, $k = 37.8$. The angular dispersion is of $S = 13.2°$, suggesting, with reserves, that indeed the Corcovado sill averages secular variation. This paleomagnetic mean direction is discordant with respect to the expected direction ($D = 357°$, $I = 6.3°$), which was obtained using the geomagnetic pole for South America of 85.9°N, 151°E ($\alpha_{95} = 2°$, $k = 93.6$) at 10 Ma (*Besse and Courtillot, 2003*). The Corcovado sill thus appears to be rotated counter-clockwise about 26.4° ± 11.3° with respect to stable South America. We submit, however, that 6 sites of uniform polarity in a single cooling unit are insufficient to average secular variation.

In a more conservative approach, we considered the 14 sites east of the Sabanalarga fault, and bounded on the east by the Cascajosa fault. We reported a mean paleomagnetic direction in a combination of coordinate systems of $D = 336.6°$, $I = 17.4°$ ($\alpha_{95} = 11.7°$, $k = 12.45$, $n = 14$). Our data thus indicate a relatively coherent mode of rotation about a vertical axis in the study area, with a counter-clockwise rotation of 20.2° ± 10.7°. This behavior slightly differs from the findings of *MacDonald (1980)* and *MacDonald et al. (1996)* being of a smaller magnitude. The remaining four sites, located west of the Sabanalarga fault (or rather on the foothills), may reflect clockwise rotation because the directions are to the NNE and shallow. Due to only four sites are reported in this area, we tentatively conclude that the sites reflect some structural complexity linked to their close proximity to the fault trace.

These findings indicate that the obduction of the Cañas Gordas terrane over the northwestern terranes of the north Andean block (*Cediel et al., 2003*) may be tentatively explained by rotations of the hypabyssal rocks of the Combia event within the Amagá basin, but the available data are inconclusive. The discordant directions in the block bounded by the Sabanalarga and Cascajosa faults may also reflect rotation about a local axis, not rotation of the entire basin. In addition, our data show that the behavior of the faults associated to the Cauca-Romeral fault system and its post Mio-Pliocene activity

(*Hutchings et al., 1981*; *Suter et al., 2008*; *Sierra et al., 2012*) must be responsible for the local tilting of the hypabyssal rocks of the Combia event, evident in the geomorphology.

7. CONCLUSIONS

The conditions of formation and crystallization of the hypabyssal rocks of the Combia event were varied, it is indicated by various types of rock that do not display deformational features at the sample level. The magnetization and magnetic susceptibility of these rocks are controlled by soft materials with low-coercivity components, which are linked to magnetite or titanomagnetite with primary origin.

Petrographic and AMS data show that hypabyssal rocks of the Combia do not present deformed features in ductile state. Some hypabyssal rocks of the Combia event may have intruded deformed sedimentary rocks, which indicates that part of the host rock (Amagá Formation) was deformed before ~10 Ma (age of the Combia event). The hypabyssal rocks of the Combia event exhibit a coherent mode of counterclockwise rotation about a vertical axis, indicated by the paleomagnetic directions located in the block between the Sabanalarga and Cascajosa faults. Similarly, the obduction of the Cañas Gordas terrane over the northwestern margin of the north Andean block may be tentatively explained by rotations in the Amagá basin; the discordant paleomagnetic directions, however, may also be explained by local-axis rotations that do not involve the entire basin. The post-Mio-Pliocene activity along the Cauca-Romeral fault system may be related to rotations and local tilting recorded in the hypabyssal rocks of the Combia event located in the central part of the Amagá basin.

Acknowledgements: The authors thank the research department of EAFIT university, the company Konica Minerales S.A and the staff of the "Laboratorio de paleomagnetismo de la Universidad Nacional Autónoma de México UNAM, CGEO-Querétaro". Field support and assistance by Daniela Cardona, Daniel Gómez, Daniel Bedoya, Esteban Gómez, Nicolas Estrada, Carlos Errazuriz and Estefania Cardona was crucial. Comments by the reviewers Bernard Henry and Germán Bayona improved the manuscript.

References

Acosta C.A., 1978. El graben interandino Colombo-Ecuatoriano (Fosa Tectónica del Cauca Patía y el corredor Andino-Ecuatoriano). *Boletín de Geología Universidad Industrial de Santander*, **12**, 63–75 (in Spanish).

Alfonso C.A., Sacks P.E., Secor D.T., Rine J. and Perez V., 1994. A tertiary fold and thrust belt in the Valle del Cauca Basin, Colombian Andes. *J. South Am. Earth Sci.*, **7**, 387–402.

Barrero D., Pardo A., Vargas C.A. and Martinez J.F., 2007. *Colombian Sedimentary Basins: Nomenclature, Boundaries and Petroleum Geology, a New Proposal*. ANH and B&M Exploration Ltd., Bogotá, Colombia.

Besse J. and Courtillot V., 2003. Correction to "Apparent and true polar wander and the geometry of the geomagnetic field over the last 200 Myr". *J. Geophys. Res.,* **108(B10)**, 2469, DOI: 10.1029/2003JB002684.

Blanco-Quintero I.F., García-Casco A., Toro L.M., Moreno M., Ruiz E.C., Vinasco C.J., Cardona A., Lázaro C. and Morata D., 2014. Late Jurassic terrane collision in the northwestern margin of Gondwana (Cajamarca complex, eastern flank of the Central Cordillera, Colombia). *Int. Geol. Rev.*, **56**, 1852–1872, DOI: 10.1080/00206814.2014.963710.

Borrero C. and Toro-Toro L.M., 2016. Vulcanismo de afnidad adaquítica en el miembro inferior de la Formación Combia (Mioceno tardío) al sur de la subcuenca de Amaga, noroccidente de Colombia. *Boletín de Geología*, **38**, 87–100 (in Spanish).

Butler R.F., 1992. *Paleomagnetism: Magnetics Domains to Geologic Terranes*. Blackwell Scientific Publications, Boston, MA.

Calle B., González H., De La Peña D., Escorce E., Durango M. et al., 1980. *Mapa geológico preliminar: República de Colombia. Plancha 166, Jericó, Escala 1:100000*. Servicio Geológico Colombiano, Bogotá, Colombia.

Calle B. and González H. 1980. *Geología y geoquímica de la plancha 166, Jericó Escala 1:100000, Memoria explicative.* Servicio Geológico Colombiano, Bogotá, Colombia (in Spanish).

Case J.E., Duran L.G., López A. and Moore W.R., 1971. Tectonic investigations in Western Colombia and Eastern Panama. *Geol. Soc. Am. Bull*, **82**, 2685–2712.

Cediel F., Shaw R.P. and Cáceres C., 2003. Tectonic assembly of the Northern Andean Block. In: Bartolini C., Buffler R. and Blickwede J. (Eds), *The Circum-Gulf of México and Caribbean: Hydrocarbon Habitats, Basin Formation and Plate Tectonics*. American Association of Petroleum Geologists Memoir, **79**, 815–848.

Chadima M. and Jelínek V., 2009. *Anisoft 4.2. Anisotropy Data Browser for Windows*. AGICO Inc., Brno, Czech Republic.

Chicangana G., 2005. The Romeral fault system: A shear and deformed extinct subduction zone between oceanic and continental lithospheres in Northwestern South America. *Earth Sci. Res.,* **9**, 51–66.

Cortes M. and Angelier J., 2005. Current states of stress in the northern Andes as indicated by focal mechanisms of earthquakes. *Tectonophysics*, **403**, 29–58, DOI: 10.1016/j.tecto.2005.03.020.

Dragoni M., Lanza R. and Tallarico A., 1997. Magnetic anisotropy produced by magma flow: theoretical model and experimental data from Ferrar dolerite sills (Antarctica). *Geophys. J. Int*., **128**, 230–240.

Dunlop D.J., 2002. Theory and application of the Day plot (Mrs/Ms versus Hcr/Hc). 1. Theoretical curves and tests using titanomagnetite data*. J. Geophys. Res.*, **107(B3)**, 2056, DOI: 10.1029/2001JB000486.

Duque-Caro H., 1990. The Choco block in the northwestern corner of South America: Structural, tectonostratigraphic, and paleogeographic implications. *J. South Am. Earth Sci.*, **3**, 71–84.

Ego F. and Sébrier M., 1995. Is the Cauca-Patía and Romeral Fault System left or right-lateral? *Geophys. Res. Lett.*, **22**, 33–36.

Fisher R.A., 1953. Dispersion on a sphere. *Proc. R. Soc. London A*, **217**, 295–305.

Gansser A., 1973, Facts and theories on the Andes. *J. Geol. Soc. London*, **129**, 93–131.

González H., 2001. *Mapa geológico del departamento de Antioquia. Geología, recursos minerales y amenazas potenciales, Escala 1:400000, Memoria explicative*. Instituto Nacional de Investigaciones Geológico Mineras, Bogotá, Colombia (in Spanish).

González H., 2010. *Geoquimica, Geocronologia de las unidades litologicas asociadas al sistema de fallas Cauca-Romeral, Sector Centro-Sur*. Proyecto Cordillera Occidental, Tomo I. Servicio Geológico Colombiano, Bogotá, Colombia (in Spanish).

Grosse E., 1926. *Mapa geológico de la parte occidental de la Cordillera Central entre el río Arma y Sacaojal, 1:50000, El terciario Carbonífero de Antioquia*. Reimer, Berlin, Germany (in Spanish).

Hutchings L., Turcotte T., McBride J. and Ochoa H., 1981. Microseismicity along and near the Dolores Shear Zone in Antioquia, Colombia. *Revista CIAF*, **6(1–3)**, 243–256.

Hrouda F., 1982. Magnetic anisotropy of rocks and its application in geology and geophysics. *Geophys. Surv.*, **5**, 37–82.

Jelínek V., 1977. *The Statistical Theory of Measuring Anisotropy of Magnetic Susceptibility of Rocks and Its Application*. Geofyzika, Brno, Czech Republic.

Jelínek V., 1981. Characterization of the magnetic fabric of rocks. *Tectonophysics*, **79**, T63–T67.

Kammer A., 1993. Las fallas de Romeral y su relación con la tectónica cordillera central. *Geología Colombiana*, **18**, 27–46 (in Spanish).

Kirschvink J.L., 1980. The least-squares line and plane and the analysis of paleomagnetic data: examples from Siberia and Morroco. *Geophys. J. R. Astron. Soc.*, **62**, 699–718.

Kono M., 1980. Statistics of paleomagnetic inclination data. *J. Geophys. Res.*, **85(B7)**, 3878–3882.

Leal-Mejía H., 2011. *Phanerozoic Gold Metallogeny in the Colombian Andes: A Tectono-Magmatic Approach.* PhD Thesis, University of Barcelona, Barcelona, Spain.

Liss D., Hutton D.H.W. and Owens W.H., 2002. Ropy flow structures: a neglected indicator of magma-flow direction in sills and dikes. *Geology*, **30**, 715–718.

López A., Sierra G.M. and Ramírez D., 2006. Vulcanismo Neógeno en el Suroccidente Antioqueño y sus implicaciones tectónicas. *Boletín de Ciencias de la Tierra*, **27**, 27–42 (in Spanish).

MacDonald W.D., 1980. Anomalous paleomagnetic directions in the Late Tertiary andesitic intrusions of the Cauca Depression, Colombian Andes. *Tectonophysics*, **68**, 339–348.

MacDonald W.D., Estrada J., Sierra G. and González H., 1996. Late Cenozoic tectonics and paleomagnetism of North Cauca Basin intrusions, Colombian Andes: Dual rotation modes. *Tectonophysics*, **261**, 277–289.

Mann P. and Corrigan J., 1990. Model for late Neogene deformation in Panama. *Geology*, **18**, 558–562.

Mann P. and Kolarsky R.A., 1995. East Panama deformed belt: Structure, age, and neotectonic significance. In: Mann P. (Ed.), *Geologic and Tectonic Development of the Caribbean Plate Boundary in Southern Central America*. The Geological Society of America, Boulder, CO, 111–130.

Marriner G.F. and Millward D., 1984. Petrochemistry of Cretaceous to recent vulcanism in Colombia. *J. Geol. Soc. London*, **141**, 473–486.

Maya M. and González H., 1995. Unidades litodémicas de la Cordillera Central de Colombia. *Boletín Geológico de Ingeominas*, **35(2–3)**, 43–57 (in Spanish).

McElhinny M.W., 1964. Statistical significance of the fold test in paleomagnetism. *Geophys. J. R. Astron. Soc*., **8**, 33–40.

McCourt W.J., 1984. *The Geology of the Central Cordillera in the Department of Valle del Cauca, Quindío and NW Tolima*. British Geological Survey Report, **84**, 8–49.

Molnar P. and Sykes L.R., 1969. Tectonics of the Caribbean and Middle America regions from focal mechanisms and seismicity. *Geol. Soc. Am. Bull*., **80(9)**, 1639–1684, DOI: 10.1130/0016-7606(1969)80[1639: TOTCAM]2.0.CO;2.

Montes C., Bayona G., Cardona A., Buchs D.M., Silva C.A., Morón S., Hoyos N., Ramírez D.A., Jaramillo C.A. and Valencia V., 2012. Arc-continent collision and orocline formation: Closing of the Central American seaway. *J. Geophys. Res*., **117**, B04105, DOI: 10.1029 /2011JB008959.

Montes C., Cardona A., Jaramillo C., Pardo A., Silva J.C., Valencia V., Ayala C., Pérez-Angel L.C., Rodriguez-Parra L.A., Ramirez V. and Niño H., 2015. Middle Miocene closure of the Central American Seaway. *Science*, **348(80)**, 226–229.

Murill, S., 1998. *Petrografía de las areniscas de la secuencia Quebrada La Sucia-Mina Palomos Miembro Inferior de la Formación Amagá*. Tesis de Pregrado. Universidad Eafit, Medellín, Colombia (in Spanish).

Peters C. and Dekkers M.J., 2003. Selected room temperature magnetic parameters as a function of mineralogy, concentration and grain size. *Phys. Chem. Earth*, **28**, 659–667.

Pindell J. and Kennan L., 2009. Tectonic evolution of the Gulf of Mexico, Caribbean and northern South America in the mantle reference frame: an update. *Geol. Soc. London Spec. Publ.*, **328**, 1–55.

Restrepo J.J, Toussaint J.F. and González H., 1981. Edades Mio-Pliocenas del magmatismo asociado a la Formación Combia, Departamentos de Antioquia y Caldas, Colombia. *Geología Norandina*, **3**, 22–26 (in Spanish).

Ribeiro J., Sant'Ovaia H., Gomes C., Ward C. and Flores D., 2015. Mineralogy and magnetic parameters of materials resulting from the mining and consumption of coal from the Douro coalfield, northwest Portugal. In: Stracher G.B., Prakash A. and Sokol E.V. (Eds), *Coal and Peat Fires: A Global Perspective*. Elsevier, Amsterdam, The Netherlands.

Rochette P., 1987. Magnetic susceptibility of the rock matrix related to magnetic fabric studies. *J. Struct. Geol*., **9**, 1015–1020.

Rochette P., Jackson J. and Aubourg C., 1992. Rock magnetism and the interpretation of ansisotropy of magnetic susceptibility. *Rev. Geophys*., **30**, 209–226.

Rochette P., Aubourg C. and Perrin M., 1999. Is this magnetic fabric normal? A review and case studies in volcanic formations. *Tectonophysics*, **307**, 219–234.

Rodriguez-Jimenez J., 2010. *Fábrica y emplazamiento de la Diorita de Pueblito, NW Cordillera Central de Colombia: análisis de fábrica magnética y mineral*. Tesis de maestría, Universidad Nacional de Colombia, Medellín, Colombia (in Spanish).

Sierra G.M. 1994. *Structural and Sedimentary Evolution of the Irra Basin, Northern Colombian Andes*. Master Thesis, State University of New York, Binghamton, NY.

Sierra G.M. and Marín-Cerón M.I., 2011. Amagá, Cauca and Patía Basins. In: Cediel F. (Ed), *Petroleum Geology of Colombia, 2*. Fondo Editorial Universidad EAFIT, Medellín, Colombia.

Sierra G.M, Marín-Cerón M.I. and MacDonald W.D., 2012. Tectonic evolution of the Irra Pull-Apart basin. Evidences of slip reversals on the Romeral Fault zone, Northern part of Andean Central Cordillera, Colombia. *Boletín de Ciencias de la Tierra*, **32**, 143–159.

Silva J.C., Sierra G.M. and Correa L.G., 2008. Tectonic and climate driven fluctuations in the stratigraphic base level of a Cenozoic continental coal basin, northwestern Andes. *J. South Am. Earth Sci.*, **26**, 369–382.

Shagam R., 1975. The northern termination of the Andes. In: Nairn A.E.M. and Stehli F.G. (Eds), *The Ocean Basins and Margins*, **3**. Plenum Press, New York, 325–420.

Suter F., Sartori M., Neuwerth R. and Gorin G., 2008. Structural imprints at the front of the Choco-Panama indenter. *Tectonophysics*, **460**, 134–157.

Taboada A., Rivera L.A., Fuenzalida A., Cisternas A., Philip H., Bijwaard H., Olaya J. and Rivera C., 2000. Geodynamics of the Northern Andes: Subductions and intracontinental deformation (Colombia). *Tectonics*, **19**, 787–813.

Tauxe L., Bertram H.N. and Seberino C., 2002. Physical interpretation of hysteresis loops: micromagnetic modeling of fine particle magnetite. *Geochem. Geophys. Geosyst.*, **10**, 1055, DOI: 10.1029/2001GC000241.

Tarling D.H. and Hrouda F., 1993. *The Magnetic Anisotropy of Rocks*. Chapman & Hall, London, U.K.

Trenkamp R., Kellogg J.N., Freymueller J.T. and Mora H.P., 2002. Wide plate margin deformation, southern Central America and northwestern South America, CASA GPS observations. *J. South Am. Earth Sci*., **15**, 157–171.

Toro G., Restrepo J.J., Poupeau G., Saenz E. and Azdimousa A., 1999. Datación por trazas de fisión de circones rosados asociados a la secuencia volcano-sedimentaria de Irra (Caldas). *Boletín de Ciencias de la Tierra*, **13**, 28–34 (in Spanish).

Uribe-Mogollón C., 2013. *Hydrothermal Evolution of Titiribí Mining District*. Tesis de Pregrado. Universidad Eafit, Medellín, Colombia.

Van der Hilst R. and Mann P., 1994. Tectonic implications of tomographic images of subducted lithosphere beneath northwestern South America. *Geology*, **22**, 451–454.

Vargas-Jimenez C.A. and Durán-Tovar J.P, 2005. State of strain and stress in Northwestern of South America. *Earth Sci. Res. J.*, **9**, 43–50.

Van der Hammen T., 1960. Estratigrafía del Terciario y Maeschtrichiano y tectonogenesis de los Andes Colombianos. *Boletín Geológico Ingeominas*, **6(1–13)**, 67–128 (in Spanish).

Van der Voo R., 1990. The reliability of paleomagnetic data. *Tectonophysics*, **184**, 1–9.

Zijderveld J.D.A., 1967. A.C. demagnetization of rocks - analysis of results. In: Collinson D.W., Creer K.M. and Runcorn S.K. (Eds), *Methods in Rock Magnetism and Paleomagnetism*. Elsevier, Amsterdam, The Netherlands, 254–286.